

CHEMISTRY

A European Journal

A Journal of



Accepted Article

Title: From Monodisperse Thienyl- and Furylborane Oligomers to Polymers - Modulating the Optical Properties Through the Heterene Ratio

Authors: Artur Lik, Sangeth Jenthra, Lars Fritze, Lars Müller, Khai-Nghi Truong, and Holger Helten

This manuscript has been accepted after peer review and appears as an Accepted Article online prior to editing, proofing, and formal publication of the final Version of Record (VoR). This work is currently citable by using the Digital Object Identifier (DOI) given below. The VoR will be published online in Early View as soon as possible and may be different to this Accepted Article as a result of editing. Readers should obtain the VoR from the journal website shown below when it is published to ensure accuracy of information. The authors are responsible for the content of this Accepted Article.

To be cited as: *Chem. Eur. J.* 10.1002/chem.201706124

Link to VoR: <http://dx.doi.org/10.1002/chem.201706124>

Supported by
ACES

WILEY-VCH

FULL PAPER

From Monodisperse Thienyl- and Furylborane Oligomers to Polymers – Modulating the Optical Properties Through the Heterarene Ratio

Artur Lik, Sangeth Jenthra, Lars Fritze, Lars Müller, Khai-Nghi Truong, and Holger Helten*

Dedicated to Prof. Dr. Alexander C. Filippou on the occasion of his 60th birthday

Abstract: The application of our newly developed B–C coupling method by catalytic Si/B exchange is demonstrated for the synthesis of a series of triarylboranes (**1**), monodisperse thienyl- and furylborane dimers (**2**) and trimers (**9**), extended oligomers (**3**) and polymers (**3'**), as well as mixed (oligo)thienyl-/furylboranes. The structures of **1aa**^{TiP}, **1bb**^{TiP}, and **2bbb**^{Mes*}, determined by X-ray crystallography, reveal largely coplanar hetarene rings and BR₃ environments, being most pronounced in the furylborane species. Photophysical investigations, supported by TD-DFT calculations, revealed pronounced π -electron delocalization over the hetarene backbones including the boron centers. Having extended series of derivatives of varying chain lengths available, allowed us to determine the effective conjugation lengths (ECL) of poly(thienylborane)s and poly(furylborane)s, which have been reached with the highest-molecular-weight derivatives of our study. Through variation of the furan-to-thiophene ratio, the photophysical properties of these materials are effectively modulated. Significantly, higher furan contents lead to considerably increased fluorescence intensities. Compounds **1aa**^{TiP}, **1bb**^{TiP}, and **3a**^{TiP} showed the ability to bind fluoride anions. The binding process is signaled by a distinct change in their optical absorption characteristics, thus rendering these materials attractive targets for sensory applications.

Introduction

In the last few decades, π -conjugated materials have been the subject of tremendous research activity,^[1] driven by applications in electronic and optoelectronic devices such as (polymer-based) organic light-emitting diodes (OLEDs/PLEDs),^[2] field-effect transistors (OFETs),^[3] and organic photovoltaic cells (OPVs),^[4,3b] as well as biomedical^[5] and sensory applications.^[6] In recent years, organic–inorganic hybrid materials generated by doping of π systems with inorganic main group elements have emerged as versatile alternatives with special features.^[7] Conjugated organoboranes^[7-11] and organoborane polymers^[7,8,10,12-18] have attracted particular attention. The incorporation of the vacant p_{π} orbital of boron into an extended π system (p – π conjugation) causes intriguing optical and electronic properties, thus enabling applications

for organic (opto)electronics, anion or amine sensing, and bio-imaging. The combination of inherently electron-deficient trivalent borane moieties with electron-rich organic π systems results in the formation of donor–acceptor arrays. Thiophene, a ubiquitous building block in organic electronic materials in general,^[19] has proved particularly useful for this purpose.^[10,11,13-15] For instance, Jäkle and Marder and co-workers presented dithienylboranes **1aa**^{Mes*} and **1aa**^{FMes} and bisboranes **2aaa**^{Mes*} and **2aaa**^{FMes}, which feature extended conjugated π systems involving largely coplanar thiophene rings and the boron centers (Figure 1).^[14] The bulky aromatic side groups, 2,4,6-tri-*tert*-butylphenyl (supermesityl, Mes*; R = *t*Bu) and 2,4,6-tris(trifluoromethyl)phenyl (fluoromesityl, FMes; R = CF₃), adopt a nearly perpendicular arrangement to this π plane and provide kinetic stabilization, thus making these species chemically very robust. Compounds **1aa**^{FMes} and **2aaa**^{FMes} and also the *B*-mesityl substituted derivative **1aa**^{Mes} (R = Me) by Miyasaka, Kobayashi, and Kawashima^[11] are able to bind and detect fluoride anions via an optical response. Recently, Jäkle et al. reported the synthesis of poly(thienylborane) **3a**^{Mes*} and related polymers comprising oligothiophene building blocks by Sn/B exchange or Stille cross-coupling polycondensation, respectively.^[15]

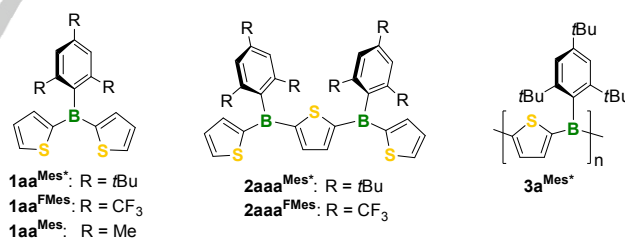


Figure 1. Dithienylboranes **1aa**^{Mes*}, **1aa**^{FMes}, **1aa**^{Mes}, thienylborane dimers **2aaa**^{Mes*}, **2aaa**^{FMes}, and poly(thienylborane) **3a**^{Mes*}.

In contrast to thiophene, the use of furan as a component for π -conjugated materials is significantly less well explored. The general value of furan-based materials for organic electronics has been recognized only quite recently, although such compounds show several favorable features and they are in some respect complementary to their well-established thiophene congeners.^[20,21] Significantly, different from most other components of organic electronic materials, furan rings are biodegradable and can be obtained from entirely renewable resources. The combination of boron with furan moieties, however, has been largely unexplored so far.^[11,22]

[*] A. Lik, S. K. Jenthra, L. Fritze, L. Müller, K.-N. Truong, Dr. H. Helten
Institute of Inorganic Chemistry, RWTH Aachen University
Landoltweg 1, 52056 Aachen (Germany)
E-mail: holger.helten@ac.rwth-aachen.de
<http://www.ac.rwth-aachen.de/extern/helten/index.html>

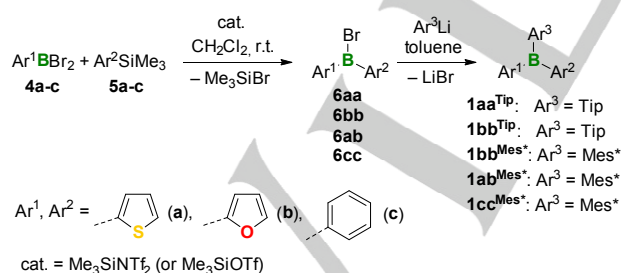
Supporting information for this article is given via a link at the end of the document.

FULL PAPER

Recently, we communicated the development of a highly efficient, environmentally benign method for the formation of B–C bonds using a novel catalytic Si/B exchange condensation approach and demonstrated its application to the synthesis of arylborane molecules, oligomers, and polymers, including the first oligo- and poly(furylborane)s.^[23,24] Herein, we report full details of these studies and an extension thereof to longer monodisperse oligomers, i. e., dimers and trimers, as well as mixed thienyl-/furylborane oligomers prepared by modular synthesis. This allows us to determine the effective conjugation lengths of these classes of compounds, and we demonstrate that their optoelectronic properties are effectively modulated through the heterocycle ratio. We also investigate the effect of the aromatic side group on the photophysical properties of the new materials and their ability to bind and detect F⁻.

Results and Discussion

Synthesis of triarylboranes. As outlined in our preliminary communication,^[23] in the first step of our investigations we explored the reaction between 2-(dibromophenyl)thiophene (**4a**) and 2-(trimethylsilyl)thiophene (**5a**) to give bromo-bis(thien-2-yl)borane **6aa** (Scheme 1). Some condensation was observed by ¹H NMR spectroscopy in a 1 M CH₂Cl₂ solution at ambient temperature already without an initiator added. However, the reaction did not go to completion within 12 d. Addition of catalytic amounts (5 mol%) of Me₃SiOTf yielded significant rate acceleration with 95 % conversion after 5 d. The stronger electrophilic species Me₃SiNTf₂, finally, proved to be a highly efficient catalyst: complete and selective conversion to **6aa** was observed with 5 mol% of Me₃SiNTf₂ at ambient temperature within 72 min. Analogous conditions were adopted to generate **6bb** and the new, mixed-substituted derivative **6ab**. Both reactions proceeded quantitatively (by ¹H NMR spectroscopy) within less than 2 h as well. The formation of the phenyl derivative **6cc** was considerably slower, and it required increased substrate concentration (4 M) and higher catalyst loading (25 mol%). Nevertheless, this reaction was fully selective, too, and afforded 95 % conversion within 3 d at room temperature.



Scheme 1. Synthesis of triarylboranes **1** via catalytic B–C coupling.

After the formation of the respective bromodiarylborane **6** was complete (or almost complete, in the case of **6cc**), the reaction mixture was evaporated to dryness, the crude product was re-dissolved in toluene and treated with a solution or suspension of the

appropriate aryllithium reagent to furnish the kinetically stabilized triarylboranes **1**. In the cases of **6aa** and **6bb**, TipLi (Tip = 2,4,6-triisopropylphenyl, triptyl) was used, which afforded the air- and moisture-stable products **1aa**^{Tip} and **1bb**^{Tip}. As our further investigations revealed that longer furylborane oligomers were water-sensitive despite having the sterically demanding Tip group attached to the boron center (see below), we additionally derivatized **6bb** with the even bulkier Mes*Li to obtain **1bb**^{Mes*}. The mixed-substituted species **6ab** was derivatized with Mes*Li as well to give the stabilized triarylborane **1ab**^{Mes*}. Only the diphenyl derivative **1cc**^{Mes*} was found to be air- and moisture-sensitive in spite of the Mes* group at boron; it decomposed gradually within 24 h under air (Figure S34, SI). However, we succeeded in isolating **1cc**^{Mes*} in pure form by re-crystallization.

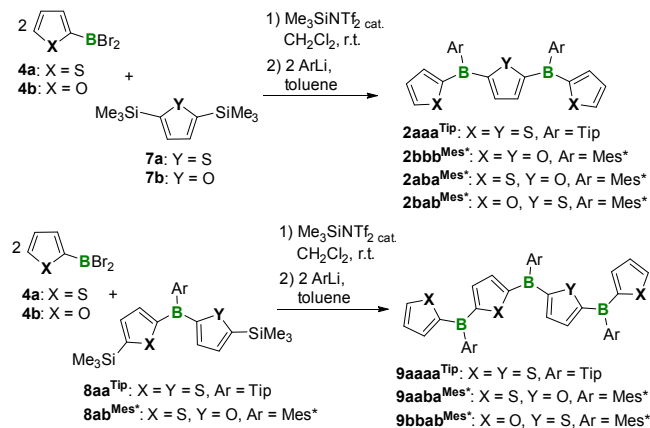
All other triarylboranes **1** were purified by column chromatography on silica and isolated in moderate to good yields (35–69%) as colorless crystalline solids. Their constitution was unambiguously ascertained by ¹H, ¹¹B, and ¹³C NMR spectroscopy, mass spectrometry, and single-crystal X-ray diffraction. In the case of **1ab**^{Mes*}, however, the quality of the X-ray data obtained was too poor to allow the discussion of structural parameters. The ¹¹B NMR resonance of compound **1ab**^{Mes*} appears at a chemical shift of 50.2 ppm, which is intermediate between that of **1aa**^{Tip} (56.1 ppm) and **1bb**^{Mes*} (47.7 ppm) or **1bb**^{Tip} (48.6 ppm), respectively. Compared to the resonance of **1cc**^{Mes*} (67.6 ppm), these signals are at significantly higher field, indicating more effective π-electron donation from the heteroaromatic rings to the vacant p_z orbital on boron. The ¹H NMR spectrum of **1bb**^{Mes*} showed broad resonances for the protons at the furan rings (see Supporting Information, Figure S26), and the spectrum of **1ab**^{Mes*} showed broadened resonances for the furyl and the thienyl protons (Figure S23, SI). This was not observed for **1bb**^{Tip} (Figure S29, SI). Presumably, this is a result of the hindered rotation of the rings in the supermesityl derivatives **1bb**^{Mes*} and **1ab**^{Mes*} in solution at ambient temperature, in contrast to **1bb**^{Tip}.

Synthesis of monodisperse oligomers. In order to systematically investigate the effect of chain elongation on the photophysical properties of linear extended thienyl- and furylboranes and also mixed species, we prepared a series of monodisperse oligomers (Scheme 2). The bisboranes **2**, which can be regarded as hetarylborane “dimers”, were synthesized by the reaction of a 2,5-bis(trimethylsilyl)hetarene **7a** or **7b** with two equivalents of either **4a** or **4b** in CH₂Cl₂ at room temperature in the presence of 5 mol% of Me₃SiNTf₂, and subsequent post-modification with TipLi or Mes*Li in toluene, respectively. The products **2aaa**^{Tip}, **2bbb**^{Mes*}, **2aba**^{Mes*}, and **2bab**^{Mes*} were isolated by column chromatography on silica, and their identity was unambiguously ascertained by multinuclear NMR spectroscopy and mass spectrometry. The structure of **2bbb**^{Mes*} in the solid-state was additionally determined by a single-crystal X-ray diffraction study.

The ¹¹B{¹H} resonances of **2aaa**^{Tip} (58 ppm) and **2bbb**^{Mes*} (49 ppm) appeared in the same range as those of their respective monoborane congeners, **1aa**^{Tip} and **1bb**^{Mes*}, however, the signals were significantly broadened (FWHM = 2980 for **2aaa**^{Tip} and 2120 Hz for **2bbb**^{Mes*}) as an effect of chain elongation. Although the mixed derivatives **2aba**^{Mes*} and **2bab**^{Mes*} both contain two boron

FULL PAPER

atoms in distinct chemical environment, they each show only one signal in their $^{11}\text{B}\{^1\text{H}\}$ NMR spectra ($\delta_{\text{B}} = 51$ ppm for **2aba**^{Mes*} and $\delta_{\text{B}} = 49$ ppm for **2bab**^{Mes*}), most likely a result of the broadened signal patterns. Furthermore, an overall increase in the ratio of furan to thiophene rings leads to a slight highfield shift of the ^{11}B signal (from **2aba**^{Mes*} to **2bab**^{Mes*} by ca. 2 ppm).



Scheme 2. Synthesis of monodisperse hetarylborane oligomers.

The synthesis of the “trimers” **9** required prior preparation of disilylated compounds **8**. This was done via dilithiation of the appropriate triarylborane **1** and subsequent reaction with Me_3SiCl (2 equiv.). Compounds **8** were then treated with two equivalents of **4** at ambient temperature in a catalytic reaction using $\text{Me}_3\text{SiNTf}_2$ (Scheme 2). Post-modification with TipLi or Mes^*Li afforded **9**. The derivatives **9aaaa**^{Tip} and **9aaba**^{Mes*} were isolated by column chromatography, and their constitution was unambiguously ascertained by NMR spectroscopy and mass spectrometry. The $^{11}\text{B}\{^1\text{H}\}$ resonance of **9aaaa**^{Tip} (57 ppm) was in the expected range and further broadened (FWHM = 3050 Hz) compared to those of the “dimers” and “monomers”; for **9aaba**^{Mes*} the resonance was not detected. The formation of **9bbab**^{Mes*} was evidenced by mass spectrometry ($m/z = 1051.1$; see SI, Figure S127), however, the product suffered from decomposition during the chromatographic work-up (see SI, Figures 62 – 64).^[25]

Structural studies. The solid-state structures of **1aa**^{Tip}, **1bb**^{Tip}, **1bb**^{Mes*}, **1cc**^{Mes*}, and the furylborane dimer **2bbb**^{Mes*} have been determined by single-crystal X-ray diffraction (Figure 2 and Table 1; the molecular structures of **1bb**^{Mes*} and **1cc**^{Mes*} have been displayed in our previous communication^[23]). In each of these compounds the boron centers are trigonal-planar coordinated (sums of the bond angles around boron, $\Sigma(\text{BC}_3)$, ca. 360° each). The Tip/Mes^* substituents are nearly perpendicular to the respective BC_3 plane, thus ruling out any possible π interaction of the vacant p orbital on boron with this aromatic system. Interestingly, the two Mes^* substituents of **2bbb**^{Mes*} point into opposite directions, which is different from the thienylborane dimers **2aaa**^{Mes*} and **2aaa**^{FMes} (with $^{\text{F}}\text{Mes} = 2,4,6\text{-(CF}_3)_3\text{C}_6\text{H}_2$) recently described by Jäkle and Marder wherein the aryl side groups are on the same

side of the molecule.^[14] The largely coplanar orientation of the hetaryl rings with respect to the BC_3 moiety, and to lesser extent also that of the phenyl rings in **1cc**^{Mes*}, indicate potential π conjugation between these groups over the boron center. In **1aa**^{Tip}, both thiophene rings are disordered by rotation about the B–C bonds, while in the furyl derivatives **1bb**^{Tip}, **1bb**^{Mes*}, and **2bbb**^{Mes*} the heterocycles consistently adopt all-*anti* conformation in the solid-state.

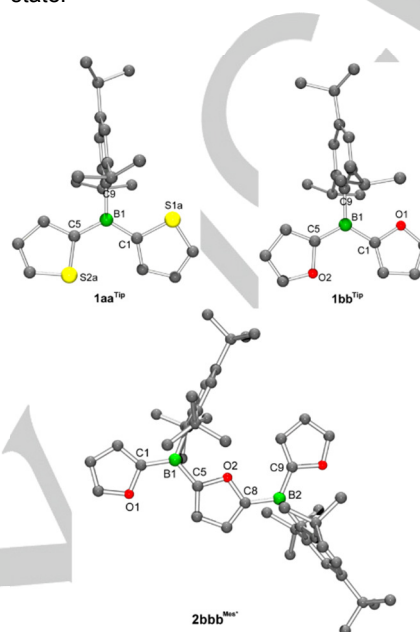


Figure 2. Molecular structures of **1aa**^{Tip}, **1bb**^{Tip}, and **2bbb**^{Mes*} in the solid state (H atoms omitted for clarity).

Table 1. Selected structural data for triarylboranes **1** and dimer **2bbb**^{Mes*}.

Compd.	Interplanar angle $\text{BC}_3\text{--Tip/Mes}^*$ [°]	Interplanar angle (hetaryl)–(hetaryl) [°]	B–C1 bond length [Å]	B–C5 bond length [Å]
1aa ^{Tip}	86.0	30.2 ^[c]	1.532(3)	1.541(3)
1bb ^{Tip}	85.6	5.1	1.529(6)	1.539(6)
1bb ^{Mes*} [a,b]	83.0, 87.0	7.7, 4.6	1.527(6), 1.542(5) ^[d]	1.529(6), 1.547(5) ^[e]
1cc ^{Mes*} [a]	83.4	43.8	1.579(3)	1.581(3)
2bbb ^{Mes*}	84.4, 88.9	6.0, 5.7	1.534(6), 1.531(6) ^[f]	1.546(6), 1.545(5) ^[g]

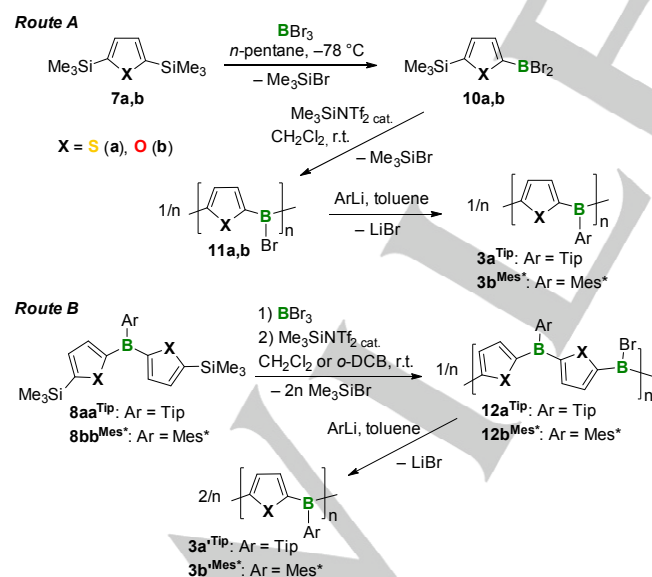
[a] Taken from ref. [23]. [b] The asymmetric unit of **1bb**^{Mes*} contains two independent molecules. [c] Mean value from the four different relative conformations of the disordered rings. [d] B2–C27. [e] B2–C31. [f] B2–C9. [g] B2–C8.

It is noteworthy that the most pronounced coplanarity of the rings is observed in the furyl derivatives **1bb**^{Tip}, **1bb**^{Mes*}, and **2bbb**^{Mes*}. The interplanar angles are 5 – 8° only. The mean twist

FULL PAPER

angle between the thiophene (Thi) planes in **1aa**^{Tip} is 30.2°, which is somewhat larger compared to those in Mes^{*}B(Thi)₂ (19.0°),^[14] ^FMesB(Thi)₂ (16.3°),^[14] and MesB(Thi)₂ (8.4 and 4.2°).^[11] The observation that the furylboranes show greater planarity than their thienylborane congeners parallels the trend found for oligofurans vs. analogous thiophene oligomers.^[21] The torsion angle between the phenyl groups in **1cc**^{Mes} is 43.8°. The lengths of the B–C bonds to the thiophene or furan substituents, respectively, in **1aa**^{Tip}, **1bb**^{Tip}, **1bb**^{Mes*}, and **2bbb**^{Mes*} are roughly in the same range, and also in the same range with those of MesB(Thi)₂ (averaged: 1.548 Å)^[11] and ^FMesB(Thi)₂ (1.541(7) and 1.526(6) Å),^[14] but significantly shorter than in Mes^{*}B(Thi)₂ (1.589(6) and 1.568(4) Å).^[14]

Polycondensation reactions. As communicated recently,^[23] we performed polycondensation reactions leading to oligo- and poly-(thienyl/furylborane)s via two different routes (Scheme 3).^[23] **Route A:** Reactions of **7a** and **7b** with one equivalent of BBr₃ at –78 °C selectively yielded the AB monomers **10a,b**, which contain both functional groups required for polycondensation (SiMe₃ and BBr₂) in one molecule. Addition of 5 mol% of Me₃SiNTf₂ to CH₂Cl₂ solutions of **10a,b**, initiated polycondensation thereof to give **11a,b**. These intermediates were subsequently derivatized with TipLi (**11a**) or Mes^{*}Li (**11b**).^[26] After aqueous work-up and purification by precipitation with ethanol this afforded the air- and moisture-stable products **3a**^{Tip} and **3b**^{Mes*}. Gel permeation chromatography (GPC), however, suggested that they were of relatively low molecular weight with narrow polydispersity (Table 2). We assume that this is a result from the observed precipitation of the intermediates **11a,b** at some point during the polycondensation process.



Scheme 3. Polycondensation reactions.

Route B: As we found that the Tip and Mes^{*} side groups impart pronounced solubility, in the next step, we decided to employ the

Tip/Mes^{*}-containing disilyl compounds **8aa**^{Tip} and **8bb**^{Mes*} as the monomers in combination with BBr₃ in analogous catalytic reactions. In the case of **8bb**^{Mes*}, we furthermore changed the solvent to the more polar 1,2-dichlorobenzene (*o*-DCB). Apparently due to the improved solubility of the macromolecular intermediates **12a**^{Tip} and **12b**^{Mes*}, the products **3a**^{Tip} and **3b**^{Mes*} were obtained with significantly increased molecular weights, corresponding to number average degrees of polymerization of 10 and 9, respectively.

Table 2. GPC data^[a] for **3a**^{Tip}, **3a**^{Tip}, **3b**^{Mes*}, and **3b**^{Mes*}.

Compd.	<i>M_n</i>	<i>M_w</i>	PDI	DP _n
3a ^{Tip}	1550	1760	1.1	4
3a ^{Tip}	3270	4100	1.3	10
3b ^{Mes*}	1880	2890	1.5	5
3b ^{Mes*}	3260	5220	1.6	9

[a] In THF, vs polystyrene standards.

Photophysical studies. All monomers **1**, dimers **2**, trimers **9**, oligomers **3**, and polymers **3'** prepared were studied by UV–vis absorption and fluorescence emission spectroscopy in THF (Table 3) which, building on related previous studies,^[14,15,23] leads to a detailed picture of the photophysical properties of such species. In the UV–vis spectra, the dihetarylborane monomers showed each an intense band at λ_{abs,max} = 315 – 325 nm and a further band at higher energy (λ_{abs,max} = 260 – 280 nm), which we assign both to π–π* transition processes based on insights gained from our time-dependent density functional theory (TD-DFT) calculations (*vide infra*). Comparison of the data for **1bb**^{Tip} and **1bb**^{Mes*} reveals a significant effect of changing the stabilizing aryl substituent from Tip to Mes^{*}. This causes a decrease in the wavelength of the lowest-energy absorption maximum by 9 nm (315 vs. 324 nm). On the other hand, the emissivity is significantly enhanced through the substituent change. Whereas **1bb**^{Tip} was found to be basically non-emissive in THF, compound **1bb**^{Mes*} showed relatively strong blue fluorescence with a quantum yield of 24 %. Presumably, this is associated with the increased rigidity of the molecules of **1bb**^{Mes*} compared to **1bb**^{Tip} due to the hindered rotation of the furan rings in the former, as evidenced by ¹H NMR spectroscopy (*vide supra*), thus favoring radiative decay processes.

In the case of the couple **1aa**^{Tip} / **1aa**^{Mes*},^[14] on the other hand, variation of the bulky aryl substituent has negligible influence on the absorption and emission characteristics of the compounds. The maximum of the lowest-energy absorption band for both derivatives appears at virtually identical wavelength. Notable fluorescence was observed for neither of them. While **1aa**^{Mes*} was described as non-emissive in THF,^[14] compound **1aa**^{Tip} showed weak fluorescence with a quantum yield of 3 %.

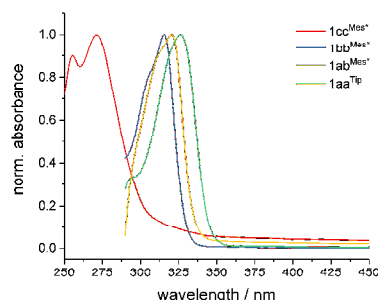
FULL PAPER

Table 3. Photophysical data^[a] for triarylboranes **1**, dimers **2**, trimers **9**, oligomers **3**, and polymers **3'**.

Compd.	$\lambda_{\text{abs,max}}$ [nm]	ϵ_{max} [10 ³ L mol ⁻¹ cm ⁻¹]	$\lambda_{\text{em,max}}$ [nm]	Φ_{F} [%]
1aa ^{Tip} [b]	325	242	410	3
1aa ^{Mes*} [c]	325	[d]	–	–
1bb ^{Tip}	324	409	–	–
1bb ^{Mes*} [b]	315	257	400	24
1ab ^{Mes*}	320	200	366	10
1cc ^{Mes*} [b]	271	194	–	–
2aaa ^{Tip}	370	239	–	–
2aaa ^{Mes*} [c]	360	[d]	–	–
2aba ^{Mes*}	360	427	–	–
2bab ^{Mes*}	361	388	–	–
2bbb ^{Mes*}	359	405	385	3
9aaaa ^{Tip}	387	358	–	–
9aaba ^{Mes*}	381	422	–	–
3a ^{Tip} [b]	409	400 ^[e]	421	1
3a' ^{Tip} [b]	412	299 ^[e]	455	1
3b ^{Mes*} [b]	407	147 ^[e]	422	70
3b' ^{Mes*} [b]	411	198 ^[e]	426	71

[a] In THF, except for **1cc**^{Mes*} (in CH₂Cl₂). [b] Taken from ref. [23]. [c] Taken from ref. [14]. [d] Not reported. [e] Per repeat unit.

Within the series of triarylboranes **1** having the same bulky aryl substituent (Mes*), the UV–vis spectra reveal a clear trend depending on nature of the conjugated aryl groups (Figure 3; due to the similarity of the spectra of **1aa**^{Tip} and **1aa**^{Mes*} it seems appropriate to include the spectrum of **1aa**^{Tip} in the graphical comparison). Here, the wavelength of the absorption maximum increases in the order: phenyl \ll furyl $<$ thienyl. The absorption band of **1cc**^{Mes*} appears at relatively high energy, evidencing rather weak conjugation between the phenyl groups, as indicated already by their orientation in the solid-state structure of **1cc**^{Mes*} (*vide supra*). The bands of the hetaryl-substituted compounds are considerably bathochromic shifted, with the maximum of the mixed-substituted derivative **1ab**^{Mes*} being right in the middle between those of **1aa**^{Tip}/**1aa**^{Mes*} and **1bb**^{Mes*}, though they are in a quite similar range. This points to comparably strong conjugation between the thienyl and the furyl groups over the boron center. The fluorescence quantum yield of 10 % for the mixed derivative **1ab**^{Mes*} fits within the trend of increasing emission intensity with increasing ratio of furan rings.

**Figure 3.** UV–vis absorption spectra of triarylboranes **1** (high-energy bands of **1aa**^{Tip}, **1ab**^{Mes*}, and **1bb**^{Mes*} omitted for clarity).

Also within the series of dimeric compounds, the thienylborane derivative **2aaa**^{Tip} absorbs at the longest wavelength ($\lambda_{\text{abs,max}} = 370$ nm). The band of its Mes* congener **2aaa**^{Mes*} is slightly blue-shifted ($\lambda_{\text{abs,max}} = 360$ nm),^[14] which correlates with the trend observed for the couple **1bb**^{Tip} / **1bb**^{Mes*}. **2aaa**^{Mes*}, the mixed dimers **2aba**^{Mes*} and **2bab**^{Mes*}, and the pure furylborane derivative **2bbb**^{Mes*} have very similar absorption characteristics with maxima at around 360 nm. Only the latter shows some fluorescence in solution.

One conclusion that can be drawn from our studies is that the furylborane species generally show significantly enhanced fluorescence compared to their thiophene congeners. This parallels the trend previously observed for purely organic oligofurans vs. oligothiophenes.^[21] Within our series of investigated compounds, the oligo- and poly(furylborane)s **3b**^{Mes*} and **3b'**^{Mes*} showed the strongest fluorescence intensities. Presumably, two effects contribute to this phenomenon: the effect of i) the presence of furan rings in the backbone and ii) the incorporation of Mes* rather than Tip as the side group.

Comparison of the UV–vis spectra for species of different chain length within each series of comparable compounds reveals considerable bathochromic shifts with increasing number of repeat units (Figure 4). This provides unequivocal evidence for effective π conjugation along the thienylborane and furylborane backbones and also along that of mixed species. With the series **1aa**^{Tip} $<$ **2aaa**^{Tip} $<$ **9aaaa**^{Tip} $<$ **3a**^{Tip} $<$ **3a'**^{Tip} and **1bb**^{Mes*} $<$ **2bbb**^{Mes*} $<$ **3b**^{Mes*} $<$ **3b'**^{Mes*} at hand, we were able to determine the effective conjugation lengths (ECL) of both poly(thienylborane)s and poly(furylborane)s by extrapolation of an exponential fit of the maximum absorption wavelengths plotted against the number of repeat units (Figure 4).^[27a] This gave an n_{ECL} of 9 repeat units for both classes of compounds. For comparison, this is smaller than the n_{ECL} values of polythiophene ($n_{\text{ECL}} = 17$),^[27a] and polyfuran ($n_{\text{ECL}} = 33$)^[27b] but larger than that of polyfluoreneborane ($n_{\text{ECL}} = 5$).^[27d] For an infinite thienylborane polymer chain our study predicts an absorption wavelength of $\lambda_{\infty} = 414$ nm, and for the limiting value of the infinite poly(furylborane) we obtain $\lambda_{\infty} = 412$ nm. Consequently, the effective conjugation lengths for both classes of polymers have been reached with **3a'**^{Tip} and **3b'**^{Mes*}, respectively.

FULL PAPER

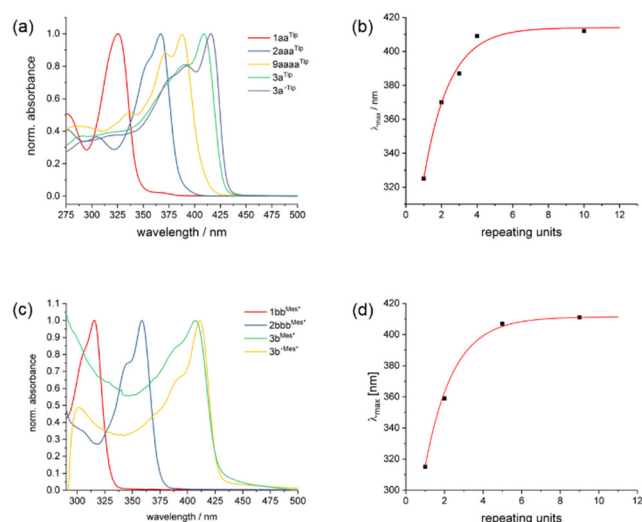


Figure 4. UV-vis absorption spectra (lowest-energy π - π^* absorption bands) and plots of the respective maximum absorption wavelengths against the number of repeat units with exponential fits to determine the effective conjugation lengths (ECL) of poly(thienylborane)s (top) and poly(furylborane)s (bottom).

The UV-vis spectra of the mixed compounds show significant red-shifts with increasing chain length as well, as shown for the series $1ab^{Mes^*} < 2aba^{Mes^*} \approx 2bab^{Mes^*} < 9aaba^{Mes^*}$ (Figure 5). This demonstrates effective π conjugation in these species between the different hetarenes and including the boron centers.

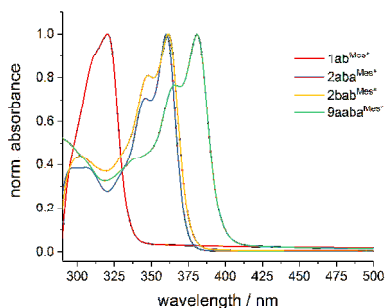


Figure 5. UV-vis absorption spectra of mixed thienyl/furylborane species $1ab^{Mes^*}$, $2aba^{Mes^*}$, $2bab^{Mes^*}$, and $9aaba^{Mes^*}$.

Electrochemical studies. The triarylboranes **1** were furthermore studied by cyclic voltammetry (CV). The CV trace of dithienylborane $1aa^{Tip}$ ($E_{1/2} = -2.50$ V) showed a reversible redox wave in the same range with that of $1aa^{Mes^*}$ ($E_{1/2} = -2.58$ V),^[14] while the difurylboranes $1bb^{Tip}$ ($E_{1/2} = -2.76$ V) and $1bb^{Mes^*}$ ($E_{1/2} = -2.83$ V) gave rise to a quasi-reversible reduction process at slightly more negative potential. The position of the half wave potentials depends on the nature of both the hetaryl groups and, to a lesser extent, the sterically demanding aryl substituent. The compounds with the bulkier Mes* substituent showed an about 70 – 80 mV more negative reduction potential than their Tip congeners. The difference of about 250 – 260 mV between the $E_{1/2}$

values of $1aa^{Mes^*}$ vs $1bb^{Mes^*}$ and $1aa^{Tip}$ vs $1bb^{Tip}$, respectively, correlates with the more electron-rich nature of furan vs thiophene. The redox wave of the mixed-substituted derivative $1ab^{Mes^*}$ ($E_{1/2} = -2.73$ V) appeared halfway between those of $1aa^{Mes^*}$ ($\Delta E_{1/2} = 150$ mV) and $1bb^{Mes^*}$ ($\Delta E_{1/2} = 100$ mV).

Computational studies. To gain deeper insight into the electronic structures of the species reported herein, we carried out DFT and TD-DFT calculations using the B3LYP functional in combination with the def2-SV(P) basis set and including the dispersion correction DFT-D3(BJ) by Grimme (see the Supporting Information, Table S8 and Figures S133 – S139, for complete results).^[28-33] As the bulky aryl substituent on boron (Ar; i.e., the side groups in the oligomers) we chose mesityl for all compounds for better comparability and computational convenience.^[34] Geometry optimization of $1aa^{Mes}$, $1bb^{Mes}$, and $1ab^{Mes}$ in the gas phase yielded structures with largely coplanar hetarene rings and BR_3 environments as observed also by crystallography for the experimental equivalents in the solid state (*vide supra*). In accordance with the solid state structures also is that the coplanarity is significantly more pronounced in the difurylborane $1bb^{Mes}$ (torsion angle between the hetaryl rings, 14.4°) than in the dithienylborane $1aa^{Mes}$ (torsion angle, 1.9°). The phenyl rings in $1cc^{Mes}$ are considerably more heavily twisted against each other (torsion angle, 47.6°).

The HOMO and the HOMO-1 of the monomeric compounds $1aa^{Mes}$, $1bb^{Mes}$, $1ab^{Mes}$, and $1cc^{Mes}$ are localized on the mesityl ring. However, excitations from these orbitals to the LUMO are predicted to be of negligible probability. According to our computations, the strongest low-energy absorption band results from a transition from the HOMO-2 to the LUMO (Figure 6). Both orbitals are characterized as π orbitals delocalized over the two (het)aryl rings,^[35] while the LUMO shows significant contribution from the p_π orbital on boron. Hence, the corresponding excitation process is characterized as a π - π^* transition associated with some degree of intramolecular charge transfer (ICT) to the boron center.

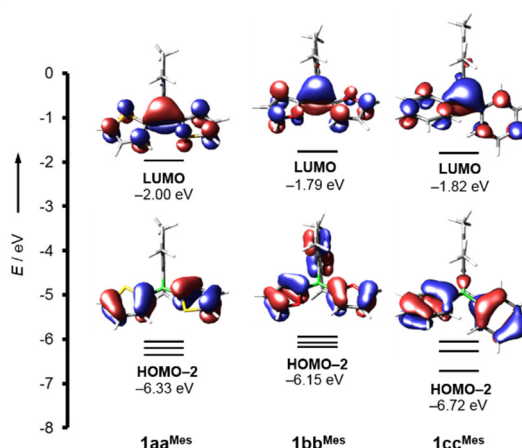


Figure 6. Orbital energy levels and plots of the LUMO and the HOMO-2 (isovalue: 0.04 au) of $1aa^{Mes}$, $1bb^{Mes}$, and $1cc^{Mes}$ (B3LYP-D3(BJ)/def2-SV(P)).

FULL PAPER

Compared to the dithienylborane **1aa**^{Mes}, in the difurylborane **1bb**^{Mes} the energy levels of all relevant orbitals are increased to approximately the same degree, which results in similar excitation energies for the two compounds (Table 4). This correlates with the more electron-rich nature of furan vs. thiophene. The calculated excitation energies are in good agreement with the experimental results, and the slight trend experimentally found for the position of the absorption maxima in the series including the mixed furyl/thienylborane species, is nicely reproduced by the computed data: **1aa**^{Mes} (316.2 nm) > **1ab**^{Mes} (309.3 nm) > **1bb**^{Mes} (305.4 nm). The diphenylborane **1cc**^{Mes} has a significantly larger HOMO-2-to-LUMO energy gap, due to a relatively lower-lying HOMO-2, which results in a shorter wavelength of the absorption maximum (286.3 nm) compared to the dihetarylboranes. Our calculations revealed for all monomeric compounds one or more closely spaced further π - π^* excitations at higher energy (Table 4). These involve a lower-lying occupied π orbital delocalized over the (het)aryl rings and the boron center and two π orbitals localized on either of the two (het)aryl rings, respectively (see SI, Figures S133 – S136). These excitations are the presumable origin of the high-energy band in the spectra of the triarylboranes investigated (*vide supra*).

Table 4. Calculated^[a] vertical singlet π - π^* excitations.

Compd.	λ [nm]	Oscillator strength f	Orbital contributions	$ c ^2$ [%]
1aa ^{Mes*}	316.2	0.3650	HOMO-2 \rightarrow LUMO	94.4
	265.7	0.0917	HOMO-5 \rightarrow LUMO	86.8
1bb ^{Mes*}	305.4	0.4886	HOMO-2 \rightarrow LUMO	75.9
			HOMO-1 \rightarrow LUMO	23.0
	258.7	0.0012	HOMO-3 \rightarrow LUMO	91.1
	233.1	0.0324	HOMO-4 \rightarrow LUMO	89.5
	230.3	0.0138	HOMO-5 \rightarrow LUMO	93.5
1ab ^{Mes*}	309.3	0.4557	HOMO-2 \rightarrow LUMO	77.8
			HOMO-1 \rightarrow LUMO	20.3
	261.5	0.1202	HOMO-4 \rightarrow LUMO	90.6
1cc ^{Mes*}	286.3	0.3061	HOMO-2 \rightarrow LUMO	94.7
	254.1	0.0806	HOMO-5 \rightarrow LUMO	91.8
2bbb ^{Mes*}	373.4	0.4885	HOMO-1 \rightarrow LUMO	68.3
9bbbb ^{Mes*}	418.8	0.6657	HOMO-1 \rightarrow LUMO	89.8

[a] TD-B3LYP-D3(BJ)/def2-SV(P).

The effect of chain elongation was investigated for furylborane oligomers,^[36] which were calculated up to the tetramer (see SI, Table S8 and Figures S137 – S139, for complete results). The bathochromic shifts of the π - π^* excitations with increasing number of repeat units are slightly overestimated by the calculations (Table 4). However, it is known that B3LYP often tends to yield somewhat lower excitation energies,^[37] and this has a greater effect on longer-wavelength transitions. Chain elongation causes a decrease of the gap between the LUMO (π^* orbital) and the relevant occupied delocalized π orbital. This leads to a change in the order of the latter and the Mes-centered orbitals (i.e., the HOMO

and the HOMO-1 in **1bb**^{Mes}). In the dimer and the trimer, **2bbb**^{Mes} and **9bbbb**^{Mes}, this becomes the HOMO-1 (Figure 7), and in the tetramer, it represents the HOMO.

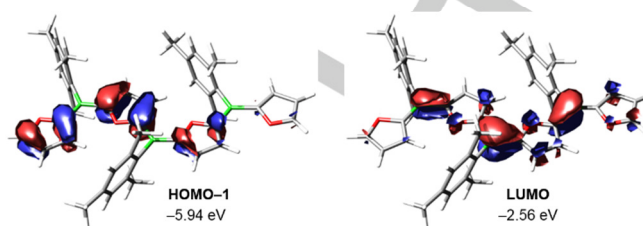


Figure 7. LUMO and HOMO-1 (isovalue: 0.04 au) of **9bbbb**^{Mes} (B3LYP-D3(BJ)/def2-SV(P)).

Fluoride sensing experiments. In order to explore the ability of our thienyl- and furylboranes to bind and detect fluoride anions,^[6,8] we performed reactions of the monomers **1aa**^{TiP}, **1bb**^{TiP}, and **1bb**^{Mes*} with tetra-*n*-butylammonium fluoride (TBAF) in THF. First, we monitored the reactions by NMR spectroscopy. Whereas the ¹¹B{¹H} NMR spectrum of **1bb**^{Mes*} remained unchanged in the presence of F⁻, in the spectra of **1aa**^{TiP} and **1bb**^{TiP}, new resonances appeared that are characteristic of four-coordinate boron species [$\delta_B = 2$ ppm (**1aa**^{TiP}), SI, Figure S21; $\delta_B = 0$ ppm (**1bb**^{TiP}), SI, Figure S31]. Encouraged by these results, we then explored the possibility to follow the putative fluoride binding processes by UV-vis spectroscopy (Figure 8a,b). Indeed, upon titration of **1aa**^{TiP} and **1bb**^{TiP} in THF with TBAF, the π - π^* absorption bands at $\lambda_{\text{abs,max}} = 325$ and 275 nm (**1aa**^{TiP}) and $\lambda_{\text{abs,max}} = 324$ and 269 nm (**1bb**^{TiP}), respectively, continuously decreased in intensity. After the addition of about two equivalents of TBAF the low-energy band was quenched completely. This is consistent with the interpretation that facile binding of fluoride to the boron center occurs; thus, leading to the formation of a borate species (see Figure 8, bottom right). Through this process, π conjugation over the boron center is effectively disrupted, hence, the corresponding π - π^* absorption bands vanish. The fluoride binding constants were determined from Benesi-Hildebrand plots as $K = 5.0 \times 10^4 \text{ M}^{-1}$ for **1aa**^{TiP} and $K = 3.9 \times 10^4 \text{ M}^{-1}$ for **1bb**^{TiP}. For the used concentration ($1.5 \times 10^{-5} \text{ M}$ in THF) both monomers showed a detection limit at a F⁻ concentration of about $1 \times 10^{-10} \text{ M}$.

We then aimed at transferring these results to the use of thienyl- and furylborane polymers **3a**^{TiP} and **3b**^{Mes*}. As in the case of the monomers, the Mes*-substituted derivative **3b**^{Mes*} showed no evidence of fluoride binding ability. Upon addition of TBAF to a solution of **3a**^{TiP}, on the other hand, the ¹¹B{¹H} NMR spectrum displayed a new resonance 0.2 ppm assigned to a borate boron center (Figure S73, SI). The π - π^* transition band in the UV-vis spectrum of **3a**^{TiP} ($\lambda_{\text{abs,max}} = 409 \text{ nm}$) continuously decreased in intensity during fluoride titration and was fully quenched when four equivalents of TBAF had been added (Figure 8c). Concomitantly, two new bands emerged at $\lambda_{\text{abs,max}} = 369$ and 294 nm.

FULL PAPER

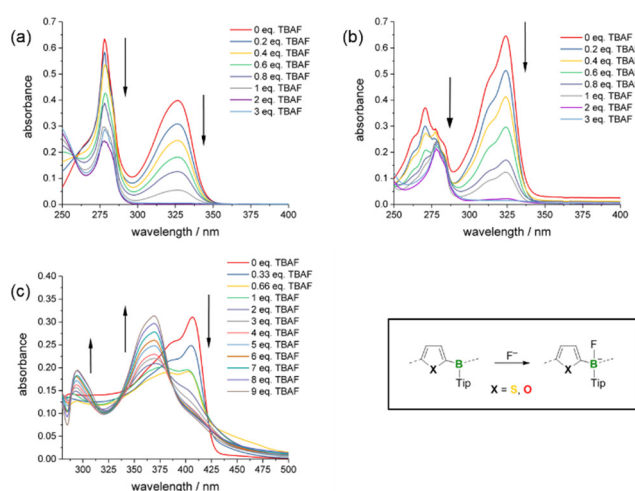


Figure 8. UV–vis absorption spectra recorded during the titration of **1aa**^{Tip} (a), **1bb**^{Tip} (b), and **3a**^{Tip} (c) with TBAF.

Conclusions

We have presented a systematic study of linear extended thienyl- and furylboranes as well as derivatives of mixed composition. Monodisperse monomers, dimers, and trimers have been prepared by modular synthesis using our newly developed catalytic Si/B exchange condensation method. Polycondensation reactions via this approach led to higher oligomers and polymers.

Having extensive series of thienyl- and furylborane oligomers and polymers of varying chain length at hand, allowed us to determine the effective conjugation lengths (ECL) of both classes of compounds, which have been reached with the highest-molecular-weight derivatives presented in this study. Extended thienyl- and furylboranes show pronounced π -electron delocalization over the hetarene backbones including the boron centers. Our photophysical investigations further showed that their absorption and emission characteristics are effectively modulated by the ratio of furan to thiophene rings incorporated. Significantly, higher furan ratios lead to considerably increased fluorescence intensities of the materials. Compounds **1aa**^{Tip}, **1bb**^{Tip}, and **3a**^{Tip} furthermore showed the ability to bind and detect fluoride anions, accompanied with a distinct change in their optical absorption characteristics. The possibility to easily monitor the binding processes by UV–vis spectroscopy demonstrates the potential use of our new materials for sensory applications.

This study demonstrates the versatile application of our catalytic B–C bond formation method for the synthesis of conjugated organoborane oligomers and polymers. It furthermore shows that furan can keep pace with thiophene groups in their use as building blocks of π conjugated materials based on triarylboranes. Currently, we are further extending our synthetic approach to access a broad range of new materials with tailored properties and functions, and we aim to elucidate mechanistic details of their formation.

Experimental Section

General procedures. All manipulations were performed under an atmosphere of dry argon using standard Schlenk techniques or in an MBraun glovebox. Solvents (dichloromethane, *n*-pentane, diethylether, toluene, and tetrahydrofuran) were dried and degassed by means of a MBraun SPS-800 solvent purification system. *o*-Dichlorobenzene was dried over CaH₂ and distilled prior to use. Deuterated solvents for NMR spectroscopy were dried and degassed at reflux over Na (C₆D₆) or CaH₂ (CDCl₃ and CD₂Cl₂) and freshly distilled prior to use. Solvents for aqueous work-up (dichloromethane, ethanol, *n*-hexane, *n*-pentane), 2-bromothiophene, tri-bromoborane, lithium bis(trifluoromethylsulfonyl)imide, bromobenzene, sulfuric acid, and magnesium turnings were purchased from commercial sources and used as received. Solutions of *n*-butyllithium (1.6 M in hexane and 2.5 M in hexane, respectively) and *t*-butyllithium (1.7 M in pentane) were purchased from Sigma Aldrich and used as received as well. Chlorotrimethylsilane, 2-bromo-1,3,5-triisopropylbenzene, thiophene and furan were commercially purchased and freshly distilled prior to use. 2-Bromofuran,^[38] trimethylsilyl bis(trifluoromethylsulfonyl)imide,^[39] 2,4,6-triisopropylphenyllithium,^[40] 2-bromo-1,3,5-tri-*tert*-butylbenzene^[41] and 2,4,6-tri-*tert*-butylphenyllithium^[14] were prepared according to methods described in the literature. Compounds **5a**, **5b**, **5c**, **4a**, **4b**, **4c**, **7a**, and **7b** were prepared according to a procedure previously described by our group.^[23] NMR spectra were recorded at 25 °C on a Bruker Avance II-400 spectrometer or on a Bruker Avance III HD spectrometer operating at 400 MHz. Chemical shifts (in ppm) were referenced to residual protic impurities in the solvent (¹H) or the deuterio solvent itself (¹³C) and reported relative to external SiMe₄ (¹H, ¹³C) or BF₃·OEt₂ (¹¹B) standards. Mass spectra were obtained with the use of a Finnigan MAT95 spectrometer employing electron ionization (EI) using a 70 eV electron impact ionization source or secondary ionization (SIMS). Elemental analysis was performed with a CHN-O-Rapid VarioEL by Heraeus. UV–vis spectra were obtained using a Jasco V-630 spectrophotometer. For fluoride titration experiments a solution of tetra-*n*-butylammonium fluoride (TBAF) in THF (1 M) was diluted to yield a solution with equivalent concentration with respect to **1aa**^{Tip}, **1bb**^{Tip}, and **3a**^{Tip}. Within a glass cuvette different equivalents of TBAF were mixed with a solution of the corresponding boron-containing compound in THF ($c = 1.5 \times 10^{-5}$ mol/L (**1aa**^{Tip}, **1bb**^{Mes*}); $c = 5.1 \times 10^{-6}$ (**3a**^{Tip})) and the reaction was monitored by determination of the UV–vis absorption spectra. As basic parameters a response of a moving average of 0.25 s, a bandwidth of 1.5 nm, and a scan speed of 1000 nm min⁻¹ were applied. Fluorescence spectra were obtained with a Jasco FP-6500 spectrofluorometer. Fluorescence quantum yields were determined against commercially available standards (**1ab**^{Mes*} against diphenylanthracene (DPA), **3a**^{Tip} and **3b**^{Mes*} against perylene). Melting points (uncorrected) were obtained using a SMP3 melting point apparatus by Stuart in 0.5 mm (o.d.) glass capillaries, which were sealed under argon. GPC chromatograms were recorded on an Agilent 1100 Series, equipped with two SDV linear N columns of 8x300 mm and 8x600 mm measures and 5 mm pore size at 30 °C against a polystyrene standard. Detection was carried out via UV signal ($\lambda = 250$ nm) and refractive index (RI), respectively. Cyclic voltammetry experiments were carried out on a PGSTAT101 analyzer from Metrohm. The three-electrode system consisted of a Pt disk as working electrode, a Pt wire as counter electrode and an Ag wire as the reference electrode. The voltammograms were recorded with ca. 10⁻³ M solutions in THF containing Bu₄N[PF₆] (0.1 M) as the supporting electrolyte. The scans were referenced after the addition of a small amount of ferrocene as internal standard. The potentials are reported relative to the ferrocene/ferrocenium couple.

General procedure for the synthesis of 1. To a solution of **5** (1 mmol) in dichloromethane (1 mL) was added TMS-NTf₂ (5 mol %) at room temperature. A solution of **4** (1 mmol) dissolved in dichloromethane (1 mL) was

FULL PAPER

added and the reaction process was monitored using ^1H NMR spectroscopy. The resulting solution was evaporated to dryness to yield crude **6**, which was subsequently re-dissolved in toluene (1.5 mL). To this solution a solution (TipLi) or a suspension (Mes*Li) of the lithiated arene (1.1 mmol) in toluene (1.5 mL) was added at -78°C . The reaction mixture was slowly warmed to room temperature and stirred over night. The resulting suspension was diluted with *n*-pentane and quenched by adding water. The organic phase was washed with brine, dried over MgSO_4 , and the solvent was removed in vacuo. The triarylborane **1cc**^{Mes*} was purified by two recrystallizations from *n*-hexane at -40°C . The other products were purified by column chromatography (silica; *n*-hexane).

General procedure for the synthesis of 2. To a solution of **7** (1 mmol) in dichloromethane (1 mL) was added TMS-NTf₂ (10 mol %) at room temperature. A solution of **4** (1 mmol) dissolved in dichloromethane (1 mL) was added and stirred over night. The resulting solution was evaporated to dryness and subsequently re-dissolved in toluene (1.5 mL). To this solution a solution (TipLi) or a suspension (Mes*Li) of the lithiated arene (1.1 mmol) in toluene (1.5 mL) was added at -78°C . The reaction mixture was slowly warmed to room temperature and stirred over night. The resulting suspension was diluted with *n*-pentane and quenched by adding water. The organic phase was washed with brine, dried over MgSO_4 , and the solvent was removed in vacuo. The products were purified by column chromatography (silica; *n*-hexane).

General procedure for the synthesis of 9. To a solution of **8** (1 mmol) in dichloromethane (1 mL) was added TMS-NTf₂ (10 mol %) at room temperature. A solution of **4** (1 mmol) dissolved in dichloromethane (1 mL) was added and stirred over night. The resulting solution was evaporated to dryness and was subsequently re-dissolved in toluene (1.5 mL). To this solution a solution (TipLi) or a suspension (Mes*Li) of the lithiated arene (1.1 mmol) in toluene (1.5 mL) was added at -78°C . The reaction mixture was slowly warmed to room temperature and stirred over night. The resulting suspension was diluted with *n*-pentane and quenched by adding water. The organic phase was washed with brine, dried over MgSO_4 , and the solvent was removed in vacuo. The products were purified by column chromatography (silica; *n*-hexane).

General procedure for the synthesis of 3 (Route A). To a solution of **7** (1 mmol) in pentane (2 mL) was added BBr₃ (1 mmol) at -78°C . The resulting suspension was stirred for 2 h maintaining -78°C . Then, the mixture was warmed to 0°C and was stirred until a solution was formed (15 min). All volatiles were removed in vacuo at 0°C to yield crude **10**, which was subsequently re-dissolved in dichloromethane (2 mL). TMS-NTf₂ (5 mol%) was added and the reaction had been stirred for three days at room temperature. After evaporating to dryness, the resulting solid residue was dispersed in toluene (3 mL). To this dispersion a solution (TipLi) or a suspension (Mes*Li) of the lithiated arene (1.25 mmol) in toluene (3 mL) was added at room temperature. The reaction mixture had been stirred for three days at room temperature. The resulting suspension was diluted with *n*-pentane and quenched by adding water. The organic phase was washed with brine, dried over MgSO_4 , and the solvent was removed in vacuo. The solid product was purified by precipitation with pentane/ethanol.

General procedure for the synthesis of 3' (Route B). To a solution of **9** (1 mmol) in *n*-pentane (10 mL) was added BBr₃ (1 mmol) at -78°C . The cooling bath was removed and the reaction had been stirred for 30 min at room temperature. After addition of dichloromethane (4 mL) the reaction had been stirred for another hour at room temperature. The resulting solution was evaporated to dryness and was subsequently re-dissolved in dichloromethane (**b**) or *o*-dichlorobenzene (**a**) (2 mL). TMS-NTf₂ (5 mol%) was added and the reaction had been stirred for three days at room temperature. After evaporating to dryness the resulting solid residue was dispersed in toluene (3 mL). To this dispersion a solution (TipLi) or a suspension (Mes*Li) of the lithiated arene (1.25 mmol) in toluene (3 mL) was added at room temperature. The reaction mixture had been stirred for three

days at room temperature. The resulting suspension was diluted with *n*-pentane and quenched by adding water. The organic phase was washed with brine, dried over MgSO_4 , and the solvent was removed in vacuo. The solid product was purified by precipitation with pentane/ethanol.

X-ray crystallographic analysis of 1aa^{Tip}, **1bb**^{Tip} and **2bbb**^{Mes*}. Suitable colorless single crystals of **1aa**^{Tip}, **1bb**^{Tip} and **2bbb**^{Mes*} were obtained by slow evaporation of hexane at ambient temperature. Data were collected on a Bruker SMART APEX CCD detector on a D8 goniometer equipped with an Oxford Cryostream 700 temperature controller at 100(2) K using graphite monochromated Mo- K_{α} radiation ($\lambda = 0.71073 \text{ \AA}$). An absorption correction was carried out semi-empirically using SADABS^[42] (min./max. transmissions = 0.4052/0.7446 (**1aa**^{Tip}; CCDC-1533828), 0.4324/0.7451 (**1bb**^{Tip}; CCDC-1533828), 0.5925/0.7452 (**2bbb**^{Mes*}; CCDC-1533828)). The structure was solved with Olex2^[43] using Direct Methods (ShelXS^[44a]) and refined with the ShelXL^[44b] refinement package by full-matrix least squares on F^2 . All non-hydrogen atoms were refined anisotropically. The hydrogen atoms were included isotropically and treated as riding. The thiophene rings in **1aa**^{Tip} are splitted. Two molecules of hexane are co-crystallized in the structure of **2bbb**^{Mes*}.

Computational methods. DFT calculations were carried out with the TURBOMOLE V7.0.1 program package.^[28] Optimizations were performed with Becke's three parameter exchange-correlation hybrid functional B3LYP^[29] in combination with the valence-double- ζ basis set def2-SV(P).^[30] The empirical dispersion correction DFT-D3 by Grimme was used including the three-body term and with Becke-Johnson (BJ) damping.^[31] The stationary points were characterized as minima by analytical vibrational frequency calculations.^[32] Vertical singlet excitations were calculated by means of time-dependent DFT^[33] using the same density functional-basis set combination as specified above.

Acknowledgements

Funding by the German Research Foundation (DFG) through the Emmy Noether Programme and the Research Grant HE 6171/4-1 and support by the COST action CM1302 (SIPs) is gratefully acknowledged. We thank Dr. K. Beckerle for GPC measurements, T. Schindler for assistance with CV measurements, Prof. Dr. U. Simon for UV-vis access, and Prof. Dr. J. Okuda for generous support and helpful discussions.

Keywords: boron • conjugated polymers • fluoride sensors • furan • thiophene

- [1] T. M. Swager, *Macromolecules* **2017**, *50*, 4867–4886.
- [2] a) A. C. Grimsdale, K. L. Chan, R. E. Martin, P. G. Jokisz, A. B. Holmes, *Chem. Rev.* **2009**, *109*, 897–1091; b) J. Liang, L. Ying, F. Huang, Y. Cao, *J. Mater. Chem. C* **2016**, *4*, 10993–11006.
- [3] a) S. Allard, M. Forster, B. Souharce, H. Thiem, U. Scherf, *Angew. Chem. Int. Ed.* **2008**, *47*, 4070–4098; *Angew. Chem.* **2008**, *120*, 4138–4167; b) P. M. Beaujuge, J. M. J. Fréchet, *J. Am. Chem. Soc.* **2011**, *133*, 20009–20029; c) C. Wang, H. Dong, W. Hu, Y. Liu, D. Zhu, *Chem. Rev.* **2012**, *112*, 2208–2267; d) J. Mei, Y. Diao, A. L. Appleton, L. Fang, Z. Bao, *J. Am. Chem. Soc.* **2013**, *135*, 6724–6746; e) H. Siringhaus, *Adv. Mater.* **2014**, *26*, 1319–1335.
- [4] a) C. Li, M. Liu, N. G. Pschirer, M. Baumgarten, K. Müllen, *Chem. Rev.* **2010**, *110*, 6817–6855; b) P.-L. T. Boudreault, A. Najari, M. Leclerc, *Chem. Mater.* **2011**, *23*, 456–469; c) H. Zhou, L. Yang, W. You, *Macromolecules* **2012**, *45*, 607–632; d) L. Dou, J. You, Z. Hong, Z. Xu, G. Li, R. A. Street, Y. Yang, *Adv. Mater.* **2013**, *25*, 6642–667.

FULL PAPER

- [5] C. Zhu, L. Liu, Q. Yang, F. Lv, S. Wang, *Chem. Rev.* **2012**, *112*, 4687–4735.
- [6] S. W. Thomas III, G. D. Joly, T. M. Swager, *Chem. Rev.* **2007**, *107*, 1339–1386.
- [7] a) X. He, T. Baumgartner, *RSC Adv.* **2013**, *3*, 11334–11350; b) A. M. Prieger, B. W. Rawe, S. C. Serin, D. P. Gates, *Chem. Soc. Rev.* **2016**, *45*, 922–953; c) H. Helten, "Conjugated Inorganic–Organic Hybrid Polymers", in *Encyclopedia of Inorganic and Bioinorganic Chemistry* (Ed.: R. A. Scott), John Wiley, Chichester, **2017**, DOI: 10.1002/9781119951438.eibc2496.
- [8] a) C. D. Entwistle, T. B. Marder, *Angew. Chem. Int. Ed.* **2002**, *41*, 2927–2931; *Angew. Chem.* **2002**, *114*, 3051–3056; b) T. W. Hudnall, C.-W. Chiu, F. P. Gabbaï, *Acc. Chem. Res.* **2009**, *42*, 388–397; c) Z. M. Hudson, S. Wang, *Acc. Chem. Res.* **2009**, *42*, 1584–1596; d) C. R. Wade, A. E. J. Broomsgrove, S. Aldridge, F. P. Gabbaï, *Chem. Rev.* **2010**, *110*, 3958–3984; e) F. Jäkle, *Chem. Rev.* **2010**, *110*, 3985–4022; f) Z. M. Hudson, S. Wang, *Dalton Trans.* **2011**, *40*, 7805–7816; g) A. Lorbach, A. Hübner, M. Wagner, *Dalton Trans.* **2012**, *41*, 6048–6063; h) K. Tanaka, Y. Chujo, *Macromol. Rapid Commun.* **2012**, *33*, 1235–1255; i) H. Zhao, L. A. Leamer, F. P. Gabbaï, *Dalton Trans.* **2013**, *42*, 8164–8178; j) A. Wakamiya, S. Yamaguchi, *Bull. Chem. Soc. Jpn.* **2015**, *88*, 1357–1377; k) F. Jäkle, *Top. Organomet. Chem.* **2015**, *49*, 297–325; l) L. Ji, S. Griesbeck, T. B. Marder, *Chem. Sci.* **2017**, *8*, 846–863; m) S.-Y. Li, Z.-B. Sun, C.-H. Zhao, *Inorg. Chem.* **2017**, *56*, 8705–8717.
- [9] a) A. G. Crawford, A. D. Dwyer, Z. Liu, A. Steffen, A. Beeby, L.-O. Pålsson, D. J. Tozer, T. B. Marder, *J. Am. Chem. Soc.* **2011**, *133*, 13349–13362; b) Y. Kim, H.-S. Huh, M. H. Lee, I. L. Lenov, H. Zhao, F. P. Gabbaï, *Chem. Eur. J.* **2011**, *17*, 2057–2062; d) Z. M. Hudson, C. Sun, M. G. Helander, Y.-L. Chang, Z.-H. Lu, S. Wang, *J. Am. Chem. Soc.* **2012**, *134*, 13930–1393; e) M. Steeger, C. Lambert, *Chem. Eur. J.* **2012**, *18*, 11937–11948; f) P. Chen, R. A. Lalancette, F. Jäkle, *Angew. Chem. Int. Ed.* **2012**, *51*, 7994–7998; *Angew. Chem.* **2012**, *124*, 8118–8122; g) Z. Zhou, A. Wakamiya, T. Kushida, S. Yamaguchi, *J. Am. Chem. Soc.* **2012**, *134*, 4529–4532; h) T. Hatakeyama, S. Hashimoto, T. Oba, M. Nakamura, *J. Am. Chem. Soc.* **2012**, *134*, 19600–19603; i) B. Neue, J. F. Aranedo, W. E. Piers, M. Parvez, *Angew. Chem. Int. Ed.* **2013**, *52*, 9966–9969; *Angew. Chem.* **2013**, *125*, 10150–10153; k) K. Matsuo, S. Saito, S. Yamaguchi, *J. Am. Chem. Soc.* **2014**, *136*, 12580–12583; m) A. N. Brown, B. Li, S.-Y. Liu, *J. Am. Chem. Soc.* **2015**, *137*, 8932–8935; n) V. M. Hertz, M. Bolte, H.-W. Lerner, M. Wagner, *Angew. Chem. Int. Ed.* **2015**, *54*, 8800–8804; *Angew. Chem.* **2015**, *127*, 8924–8928; o) X.-Y. Wang, A. Narita, X. Feng, K. Müllen, *J. Am. Chem. Soc.* **2015**, *137*, 7668–7671; S. Wang, D.-T. Yang, J. Lu, H. Shimogawa, S. Gong, X. Wang, S. K. Møllerup, A. Wakamiya, Y.-L. Chang, C. Yang, Z.-H. Lu, *Angew. Chem. Int. Ed.* **2015**, *54*, 15074–15078; *Angew. Chem.* **2015**, *127*, 15289–15293; p) L. Ji, R. M. Edkins, A. Lorbach, I. Krummenacher, C. Bruckner, A. Eichhorn, H. Braunschweig, B. Engels, P. J. Low, T. B. Marder, *J. Am. Chem. Soc.* **2015**, *137*, 6750–6753; r) Z. Zhang, R. M. Edkins, M. Haehnel, M. Wehner, A. Eichhorn, L. Mailänder, M. Meier, J. Brand, F. Brede, K. Müller-Buschbaum, H. Braunschweig, T. B. Marder, *Chem. Sci.* **2015**, *6*, 5922–5927; s) H. Hirai, K. Nakajima, S. Nakatsuka, K. Shiren, J. Ni, S. Nomura, T. Ikuta, T. Hatakeyama, *Angew. Chem. Int. Ed.* **2015**, *54*, 13581–13585; *Angew. Chem.* **2015**, *127*, 13785–13789; t) K. Suzuki, S. Kubo, K. Shizu, T. Fukushima, A. Wakamiya, Y. Murata, C. Adachi, H. Kaji, *Angew. Chem. Int. Ed.* **2015**, *54*, 15231–15235; *Angew. Chem.* **2015**, *127*, 15446–15450; u) P. Chen, X. Yin, N. Baser-Kirazli, F. Jäkle, *Angew. Chem. Int. Ed.* **2015**, *54*, 10768–10772; *Angew. Chem.* **2015**, *127*, 10918–10922; v) K. Matsuo, S. Saito, S. Yamaguchi, *Angew. Chem. Int. Ed.* **2016**, *55*, 11984–11988; *Angew. Chem.* **2016**, *128*, 12163–12167; w) A. John, M. Bolte, H.-W. Lerner, M. Wagner, *Angew. Chem. Int. Ed.* **2017**, *56*, 5588–5592; *Angew. Chem.* **2017**, *129*, 5680–5684.
- [10] Y. Ren, F. Jäkle, *Dalton Trans.* **2016**, *45*, 13996–14007.
- [11] a) C. Branger, M. Lequan, R. M. Lequan, M. Barzoukas, A. Fort, *J. Mater. Chem.* **1996**, *6*, 555–558; b) T. Noda, Y. Shirota, *J. Am. Chem. Soc.* **1998**, *120*, 9714–9715; c) Z. Yuan, J. C. Collings, N. J. Taylor, T. B. Marder, C. Jardin, J.-F. Halet, *J. Solid State Chem.* **2000**, *154*, 5–12; d) A. Sundararaman, K. Venkatasubbaiah, M. Victor, L. N. Zakharov, A. L. Rheingold, F. Jäkle, *J. Am. Chem. Soc.* **2006**, *128*, 16554–16565; e) A. Wakamiya, K. Mori, S. Yamaguchi, *Angew. Chem. Int. Ed.* **2007**, *46*, 4273–4276; *Angew. Chem.* **2007**, *119*, 4351–4354; f) A. Sundararaman, R. Varughese, H. Li, L. N. Zakharov, A. L. Rheingold, F. Jäkle, *Organometallics* **2007**, *26*, 6126–6131; g) L. Weber, V. Werner, M. A. Fox, T. B. Marder, S. Schwedler, A. Brockhinke, H.-G. Stämmler, B. Neumann, *Dalton Trans.* **2009**, *41*, 1339–1351; h) A. Wakamiya, K. Mori, T. Araki, S. Yamaguchi, *J. Am. Chem. Soc.* **2009**, *131*, 10850–10851; i) S. Miyasaka, J. Kobayashi, T. Kawashima, *Tetrahedron Lett.* **2009**, *50*, 3467–3469; j) M. Lepeltier, O. Lukoyanova, A. Jacobson, S. Jeeva, D. F. Perepichka, *Chem. Commun.* **2010**, *46*, 7007–7009; k) A. Iida, S. Yamaguchi, *J. Am. Chem. Soc.* **2011**, *133*, 6952–6955; l) C.-T. Poon, W. H. Lam, V. W.-W. Yam, *J. Am. Chem. Soc.* **2011**, *133*, 19622–19625; m) H. Braunschweig, A. Damme, J. O. C. Jimenez-Halla, C. Hörl, I. Krummenacher, T. Kupfer, L. Mailänder, K. Radacki, *J. Am. Chem. Soc.* **2012**, *134*, 20169–20177; n) H. Braunschweig, V. Dyakonov, B. Engels, Z. Falk, C. Hörl, J. H. Klein, T. Kramer, H. Kraus, I. Krummenacher, C. Lambert, C. Walter, *Angew. Chem. Int. Ed.* **2013**, *52*, 12852–12855; *Angew. Chem.* **2013**, *125*, 13088–13092; o) L. G. Mercier, W. E. Piers, R. W. Harrington, W. Clegg, *Organometallics* **2013**, *32*, 6820–6826; p) X.-Y. Wang, H.-R. Lin, T. Lei, D.-C. Yang, F.-D. Zhuang, J.-Y. Wang, S.-C. Yuan, J. Pei, *Angew. Chem. Int. Ed.* **2013**, *52*, 3117–3120; *Angew. Chem.* **2013**, *125*, 3199–3202; q) X.-Y. Wang, F.-D. Zhuang, R.-B. Wang, X.-C. Wang, X.-Y. Cao, J.-Y. Wang, J. Pei, *J. Am. Chem. Soc.* **2014**, *136*, 3764–3767; r) D. R. Levine, M. A. Siegler, J. D. Tovar, *J. Am. Chem. Soc.* **2014**, *136*, 7132–7139; s) Z. Zhang, R. M. Edkins, J. Nitsch, K. Fucke, A. Eichhorn, A. Steffen, Y. Wang, T. B. Marder, *Chem. Eur. J.* **2015**, *21*, 177–190; t) H. Braunschweig, R. D. Dewhurst, T. Kramer, *Inorg. Chem.* **2015**, *54*, 3619–3623; u) Y. Cao, J. K. Nagle, M. O. Wolf, B. O. Patrick, *J. Am. Chem. Soc.* **2015**, *137*, 4888–4891; v) S. K. Sarkar, G. R. Kumar, P. Thilagar, *Chem. Commun.* **2016**, *52*, 4175–4178; w) X. Yin, K. Liu, Y. Ren, R. A. Lalancette, Y.-L. Loo, F. Jäkle, *Chem. Sci.* **2017**, *8*, 5497–5505.
- [12] a) N. Matsumi, K. Naka, Y. Chujo, *J. Am. Chem. Soc.* **1998**, *120*, 10776–10777; b) A. Nagai, T. Murakami, Y. Nagata, K. Kokado, Y. Chujo, *Macromolecules* **2009**, *42*, 7217–7220; c) A. Lorbach, M. Bolte, H. Li, H.-W. Lerner, M. C. Holthausen, F. Jäkle, M. Wagner, *Angew. Chem. Int. Ed.* **2009**, *48*, 4584–4588; *Angew. Chem.* **2009**, *121*, 4654–4658; d) H. Li, F. Jäkle, *Angew. Chem. Int. Ed.* **2009**, *48*, 2313–2316; *Angew. Chem.* **2009**, *121*, 2349–2352; e) J. B. Heilmann, M. Scheibitz, Y. Qin, A. Sundararaman, F. Jäkle, T. Kretz, M. Bolte, H.-W. Lerner, M. C. Holthausen, M. Wagner, *Angew. Chem. Int. Ed.* **2006**, *45*, 920–925; *Angew. Chem.* **2006**, *118*, 934–939; f) I. A. Adams, P. A. Rupar, *Macromol. Rapid Commun.* **2015**, *36*, 1336–1340; g) F. Pammer, R. A. Lalancette, F. Jäkle, *Chem. Eur. J.* **2011**, *17*, 11280–11289; h) D. Marinelli, F. Fasano, B. Najjari, N. Demitri, D. Bonifazi, *J. Am. Chem. Soc.* **2017**, *139*, 5503–5519; i) a) A. W. Baggett, F. Guo, B. Li, S.-Y. Liu, F. Jäkle, *Angew. Chem. Int. Ed.* **2015**, *54*, 11191–11195; *Angew. Chem.* **2015**, *127*, 11343–11347.
- [13] a) H. Li, A. Sundararaman, K. Venkatasubbaiah, F. Jäkle, *J. Am. Chem. Soc.* **2007**, *129*, 5792–5793; b) C. Reus, F. Guo, A. John, M. Winhold, H.-W. Lerner, F. Jäkle, M. Wagner, *Macromolecules* **2014**, *47*, 3727–3735; c) X.-Y. Wang, F.-D. Zhuang, J.-Y. Wang, J. Pei, *Chem. Commun.* **2015**, *51*, 17532–17535.
- [14] X. Yin, J. Chen, R. A. Lalancette, T. B. Marder, F. Jäkle, *Angew. Chem. Int. Ed.* **2014**, *53*, 9761–9765; *Angew. Chem.* **2014**, *126*, 9919–9923.
- [15] a) X. Yin, F. Guo, R. A. Lalancette, F. Jäkle, *Macromolecules* **2016**, *49*, 537–546; b) A. Sundararaman, M. Victor, R. Varughese, F. Jäkle, *J. Am. Chem. Soc.* **2005**, *127*, 13748–13749.
- [16] For polymers with tetracoordinate boron centers in the main chain, see, e. g.: a) N. Matsumi, K. Naka, Y. Chujo, *Polym. J.* **1998**, *30*, 833–837; b) F. Matsumoto, Y. Chujo, *J. Organomet. Chem.* **2003**, *680*, 27–30; c) N. Christinat, E. Croisier, R. Scopelliti, M. Cascella, U. Röthlisberger, K.

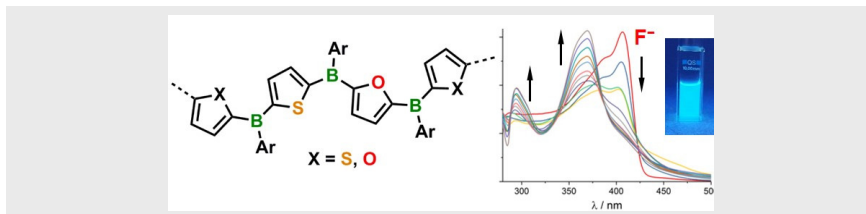
FULL PAPER

- Severin, *Eur. J. Inorg. Chem.* **2007**, 5177–5181; d) G. Meng, S. Velayudham, A. Smith, R. Luck, H. Liu, *Macromolecules* **2009**, *42*, 1995–2001; e) A. Nagai, Y. Chujo, *Macromolecules* **2010**, *43*, 193–200; f) B. Kim, B. Ma, V. R. Donuru, H. Liu, J. M. J., Fréchet, *Chem. Commun.* **2010**, 46, 4148–4150; g) S. M. Barbon, J. B. Gilroy, *Polym. Chem.* **2016**, *7*, 3589–3598.
- [17] For polymers with boron-containing conjugated side groups, see, e. g.: a) D. Reitzenstein, C. Lambert, *Macromolecules* **2009**, *42*, 773–782; b) A. Nagai, K. Kokado, J. Miyake, Y. Chujo, *Macromolecules* **2009**, *42*, 5446–5452; c) F. Pammer, F. Guo, R. A. Lalancette, F. Jäkle, *Macromolecules* **2012**, *45*, 6333–6343; d) Z. M. Hudson, D. J. Lunn, M. A. Winnik, I. Manners, *Nat. Commun.* **2014**, *5*, 3372; e) S. Novoa, J. B. Gilroy, *Polym. Chem.* **2017**, *8*, 5388–5395; f) J. Wang, B. Jin, N. Wang, T. Peng, X. Li, Y. Luo, S. Wang, *Macromolecules* **2017**, *50*, 4629–4638.
- [18] For non-conjugated polymers with boron in the main chain, see, e. g.: a) A. Staubitz, A. Presa Soto, I. Manners, *Angew. Chem. Int. Ed.* **2008**, *47*, 6212–6215; *Angew. Chem.* **2008**, *120*, 6308–6311; b) H. Dorn, R. A. Singh, J. A. Massey, A. J. Lough, I. Manners, *Angew. Chem. Int. Ed.* **1999**, *38*, 3321–3323; *Angew. Chem.* **1999**, *111*, 3540–3543; c) C. Marquardt, T. Jurca, K.-C. Schwan, A. Stauber, A. V. Virovets, G. R. Whittell, I. Manners, M. Scheer, *Angew. Chem. Int. Ed.* **2015**, *54*, 13782–13786; *Angew. Chem.* **2015**, *127*, 13986–13991; d) A. Ledoux, P. Larini, C. Boisson, V. Monteil, J. Raynaud, E. Lacôte, *Angew. Chem. Int. Ed.* **2015**, *54*, 15744–15749; *Angew. Chem.* **2015**, *127*, 15970–15975.
- [19] a) I. Osaka, R. D. McCullough, *Acc. Chem. Res.* **2008**, *41*, 1202–1214; b) A. Mishra, C.-Q. Ma, P. Bäuerle, *Chem. Rev.* **2009**, *109*, 1141–1276; c) M. E. Cinar, T. Ozturk, *Chem. Rev.* **2015**, *115*, 3036–3140.
- [20] H. Cao, P. A. Rugar, *Chem. Eur. J.* **2017**, *23*, 14670–14675.
- [21] a) O. Gidron, Y. Diskin-Posner, M. Bendikov, *J. Am. Chem. Soc.* **2010**, *132*, 2148–2150; b) U. H. F. Bunz, *Angew. Chem. Int. Ed.* **2010**, *49*, 5037–5040; *Angew. Chem.* **2010**, *122*, 5159–5162; c) B. C. Streifel, J. D. Tovar, *Encyclopedia of Polymer Science and Technology*, Wiley, New York, **2012**; d) M. S. Chen, O. P. Lee, J. R. Niskala, A. T. Yiu, C. J. Tassone, K. Schmidt, P. M. Beaujuge, S. S. Onishi, M. F. Toney, A. Zettl, J. M. J. Fréchet, *J. Am. Chem. Soc.* **2013**, *135*, 19229–19236; e) M. Jeffries-EL, B. M. Kobilka, B. J. Hale, *Macromolecules* **2014**, *47*, 7253–7271; f) X.-H. Jin, D. Sheberla, L. J. W. Shimon, M. Bendikov, *J. Am. Chem. Soc.* **2014**, *136*, 2592–2601; g) H. Cao, I. A. Brettell-Adams, F. Qu, P. A. Rugar, *Organometallics* **2017**, *36*, 2565–2572; h) L. Huo, T. Liu, B. Fan, Z. Zhao, X. Sun, D. Wei, M. Yu, Y. Liu, Y. Sun, *Adv. Mater.* **2015**, *27*, 6969–6975; i) C. H. Woo, P. M. Beaujuge, T. W. Holcombe, O. P. Lee, J. M. J. Fréchet, *J. Am. Chem. Soc.* **2010**, *132*, 15547–15549; j) Y. Xiong, J. Tao, R. Wang, X. Qiao, X. Yang, D. Wang, H. Wu, H. Li, *Adv. Mater.* **2016**, *28*, 5949–5953; k) C.-H. Tsai, A. Fortney, Y. Qiu, R. R. Gil, D. Yaron, T. Kowalewski, K. J. T. Noonan, *J. Am. Chem. Soc.* **2016**, *138*, 6798–6804; l) S. Zhen, B. Lu, J. Xu, S. Zhang, Y. Li *RSC Adv.* **2014**, *4*, 14001–14012; m) S. Zhen, J. Xu, B. Lu, S. Zhang, L. Zhao, J. Li *Electrochim. Acta.* **2014**, *146*, 666–678.
- [22] For early studies of difurylboranes, see: a) B. Wrackmeyer, H. Nöth, *Chem. Ber.* **1976**, *109*, 1075–1088; b) T. Köhler, J. Faderl, H. Pritzkow, W. Siebert, *Eur. J. Inorg. Chem.* **2002**, 2942–2946.
- [23] A. Lik, L. Fritze, L. Müller, H. Helten, *J. Am. Chem. Soc.* **2017**, *139*, 5692–5695.
- [24] We recently developed Si/B exchange polycondensation as a route to polymers with B–N linkages: a) T. Lorenz, A. Lik, F. A. Plamper, H. Helten, *Angew. Chem. Int. Ed.* **2016**, *55*, 7236–7241; *Angew. Chem.* **2016**, *128*, 7352–7357; b) O. Ayhan, T. Eckert, F. A. Plamper, H. Helten, *Angew. Chem. Int. Ed.* **2016**, *55*, 13321–13325; *Angew. Chem.* **2016**, *128*, 13515–13519; c) H. Helten, *Chem. Eur. J.* **2016**, *22*, 12972–12982; d) T. Lorenz, M. Crumbach, T. Eckert, A. Lik, H. Helten, *Angew. Chem. Int. Ed.* **2017**, *56*, 2780–2784; *Angew. Chem.* **2017**, *129*, 2824–2828; e) N. A. Riensch, A. Deniz, S. Kühl, L. Müller, A. Adams, A. Pich, H. Helten, *Polym. Chem.* **2017**, *8*, 5264–5268.
- [25] We also attempted the synthesis of a furylborane trimer (**9bbbb**). This, however, was not successful, probably due to decomposition of the intermediate formed during the catalytic reaction.
- [26] In this case Mes*Li was used rather than Tipli because we found that the derivative **3b^{TiP}** was unstable toward ethanol.
- [27] a) H. Meier, U. Stalmach, H. Kolshorn, *Acta Polym.* **1997**, *48*, 379–384; b) D. Sheberla, S. Patra, Y. H. Wijsboom, S. Sharma, Y. Sheynin, A.-E. Haj-Yahia, A. H. Barak, O. Gidron, M. Bendikov *Chem. Sci.* **2015**, *6*, 360–371; c) X.-H. Jin, D. Sheberla, L. J. W. Shimon, M. Bendikov *J. Am. Chem. Soc.* **2014**, *136*, 2592; d) P. Chen, R. A. Lalancette, F. Jäkle *J. Am. Chem. Soc.* **2011**, *133*, 8802–8805.
- [28] Turbomole: R. Ahlrichs, M. Bär, M. Häser, H. Horn, C. Kölmel, *Chem. Phys. Lett.* **1989**, *162*, 165–169.
- [29] a) P. A. M. Dirac, *Proc. R. Soc. London, Ser. A* **1929**, *123*, 714–733; b) J. C. Slater, *Phys. Rev.* **1951**, *81*, 385–390; c) A. D. Becke, *Phys. Rev. A.* **1988**, *38*, 3098–3100; d) C. Lee, W. Yang, R. G. Parr, *Phys. Rev. B* **1988**, *37*, 785–789; e) A. D. Becke, *J. Chem. Phys.* **1993**, *98*, 5648–5652.
- [30] A. Schäfer, H. Horn, R. Ahlrichs, *J. Chem. Phys.* **1992**, *97*, 2571–2577.
- [31] a) S. Grimme, J. Antony, S. Ehrlich, H. Krieg, *J. Chem. Phys.* **2010**, *132*, 154104; b) S. Grimme, S. Ehrlich, L. Goerigk, *J. Comput. Chem.* **2011**, *32*, 1456–1465.
- [32] P. Deglmann, F. Furche, R. Ahlrichs, *Chem. Phys. Lett.* **2002**, *362*, 511–518; b) P. Deglmann, F. Furche, *J. Chem. Phys.* **2002**, *117*, 9535–9538.
- [33] a) R. Bauernschmitt, R. Ahlrichs, *Chem. Phys. Lett.* **1996**, *256*, 454–464; b) R. Bauernschmitt, R. Ahlrichs, *J. Chem. Phys.* **1996**, *104*, 9047–9052; c) F. Furche, D. Rappoport, “Density functional methods for excited states: equilibrium structure and electronic spectra”, in M. Olivucci (Ed.) *Computational Photochemistry*, Vol. 16 of *Computational and Theoretical Chemistry*, ch. III., Elsevier, Amsterdam, **2005**.
- [34] This truncation appears appropriate as our results obtained for **1aa^{Mes}** and **1bb^{Mes}** are comparable to those reported in our communication^[23] for **1aa^{TiP}** and **1bb^{TiP}** and previously^[14] for **1aa^{Mes*}** and **2aaa^{Mes*}**.
- [35] In the case of **1bb^{Mes}** and **1ab^{Mes}** (SI, Figure S135), the HOMO–2 shows some mixing between the π systems of the heteraryl rings and the mesityl ring.
- [36] For thienylboranes this was not further investigated at this point as calculations on dimers **2aaa^{Mes*}** and **2aaa^{FMes}** were reported previously^[14]
- [37] a) A. Dreuw, M. Head-Gordon, *Chem. Rev.* **2005**, *105*, 4009–4037; b) D. Jacquemin, B. Mennucci, C. Adamo, *Phys. Chem. Chem. Phys.* **2011**, *13*, 16987–16998.
- [38] M. A. Keegstra, A. J. A. Klomp, L. Brandsma, *Synth. Commun.* **1990**, *20*, 3371–3374.
- [39] B. Mathieu, L. Ghosez, *Tetrahedron* **2002**, *58*, 8219–8226.
- [40] K. Ruhlandt-Senge, J. J. Ellison, R. J. Wehmschulte, F. Pauer, P. P. Power, *J. Am. Chem. Soc.* **1993**, *115*, 11353–11357.
- [41] D. E. Pearson, M. G. Frazer, V. S. Frazer, L. C. Washburn, *Synthesis* **1976**, *9*, 621–623.
- [42] SADABS: Area-Detector Absorption Correction; Siemens Industrial Automation, Inc.: Madison, WI, **1996**.
- [43] O. V. Dolomanov, L. J. Bourhis, R. J. Gildea, J. A. K. Howard, H. J. Puschmann, *J. Appl. Cryst.* **2009**, *42*, 339–341.
- [44] a) G. M. Sheldrick, *Acta Crystallogr., Sect. A* **2008**, *64*, 112–122; b) G. M. Sheldrick, *Acta Crystallogr., Sect. C* **2015**, *71*, 3–8.

FULL PAPER

Entry for the Table of Contents

FULL PAPER



A. Lik, S. Jenthra, L. Fritze, L. Müller, K.-N. Truong, H. Helten*

Page No. – Page No.

From Monodisperse Thienyl- and Furylborane Oligomers to Polymers – Modulating the Optical Properties Through the Hetero Ratio

Catalytic Si/B exchange polycondensation provided access to a series of thienyl- and furylboranes, monodisperse oligomers, and polymers. The photophysical properties of such species are effectively modulated through variation of the ratio of the heterocycles in the backbone. Careful choice of the constituent rings and the side groups leads to materials that detect fluoride anions via an optical response.